

Mclean seminar sec.11.3.3-11.5.2

2024/12/06

M1 Kensho Tanaka

11.3	Infrared array detectors	393
11.3.1	The infrared “array” revolution, <i>déjà vu</i>	393
11.3.2	The hybrid structure	397
11.3.3	Photovoltaic devices	400
11.3.4	Impurity band conduction devices	401
11.3.5	Far-infrared arrays based on germanium	403
11.3.6	Other forms of infrared arrays	404
11.4	Practical operation of infrared arrays	405
11.4.1	Linearity	405
11.4.2	Dark current and cooling	406
11.4.3	Noise sources	407
11.4.4	Quantum efficiency	408
11.4.5	Multiple outputs	408
11.4.6	Array controllers	408
11.5	Readout modes	410
11.5.1	Single-sampling	412
11.5.2	Correlated double-sampling (CDS)	413
11.5.3	Reset–read–read or Fowler sampling	413
11.5.4	Sampling up the ramp (UTR)	415
11.6	Infrared instruments	415
11.6.1	General issues	415
11.6.2	IR cameras	416
11.6.3	Infrared spectrometers	417
11.6.4	AO cameras and integral field spectroscopy	419
11.7	The impact of infrared arrays	420
11.7.1	Ground-based observing	420
11.7.2	The Stratospheric Observatory for Infrared Astronomy	421
11.7.3	IR astronomy in space	423

11.3.3 Photovoltaic devices

- Teledyne Image Sensor
 - The development of HgCdTe arrays
 - A process known as PACE-I (Producible Alternative to CdTe for Epitaxy) was used to develop HgCdTe IR arrays.
 - The percentage of Hg to Cd determines the cutoff wavelength.

G.L. Hansen et al, 1982

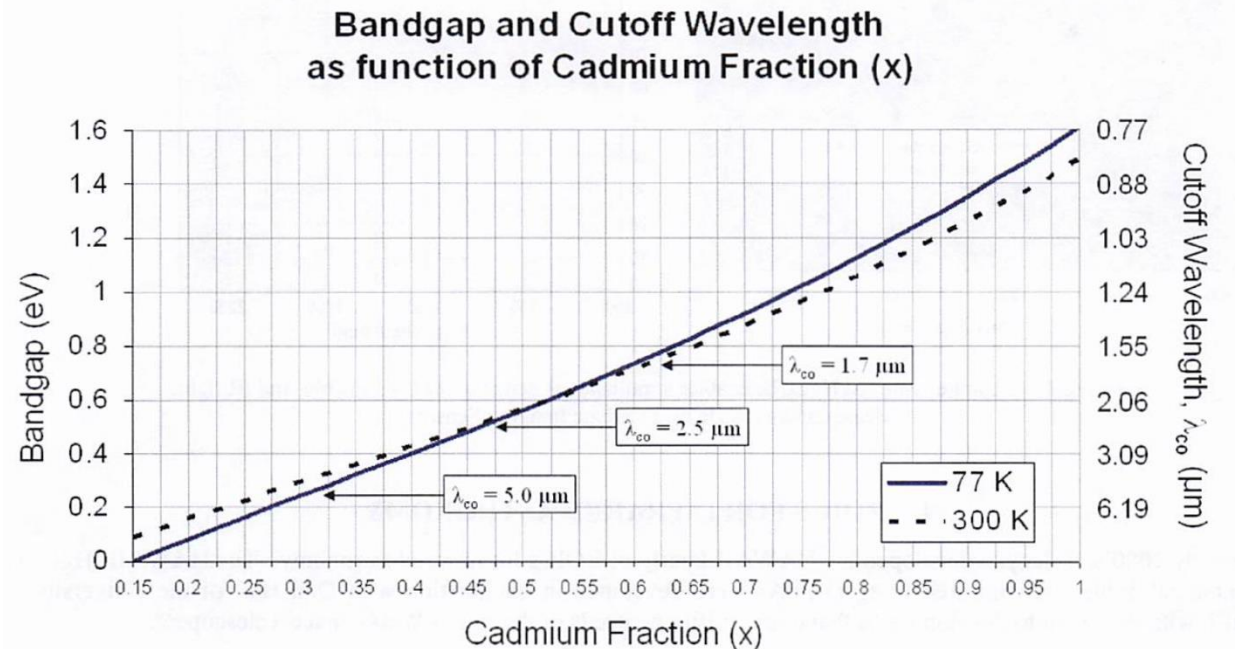
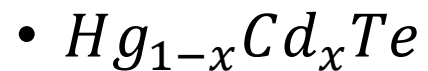


Figure 3: Bandgap and cutoff wavelength of HgCdTe as a function of the cadmium fraction

11.3.3 Photovoltaic devices

- Newer devices are made by molecular beam epitaxy (MBE)
 - Response to the visible wavelengths
 - Resistance to particle damages for space applications
 - 0.5-2.5 μm detector was developed for JWST
- Indium antimonide (InSb) photodiode
 - Available from Raytheon Vision Systems (RVS)
 - frontside illumination -> backside illumination
 - InSb arrays must be thinned to about 10 μm as the substrate is not transparent.

11.3.4 Impurity band conduction devices

- an IBC device
 - A heavily doped infrared-active layer is placed in contact with a pure (undoped) epitaxial layer (the blocking layer) so that overall **thickness of the device can be greatly reduced**.
 - The blocking layer is isolated by an oxide layer from metal contact pads.
 - Dark current due to “hopping” is prevented by the blocking layer
 - Enables much higher doping levels
 - Which permits the thin layer.
 - High QE regardless of a thin layer.
 - Do not exhibit generation-recombination noise since the collected electrons are transported over a region devoid of holes.

- QE is dependent on the concentration of the impurity atoms.
- But high concentration leads to tunneling or “hopping”.
- ➔ Only way to increase QE is to widen the active layer.
- ➔ but it causes the many operational problems.

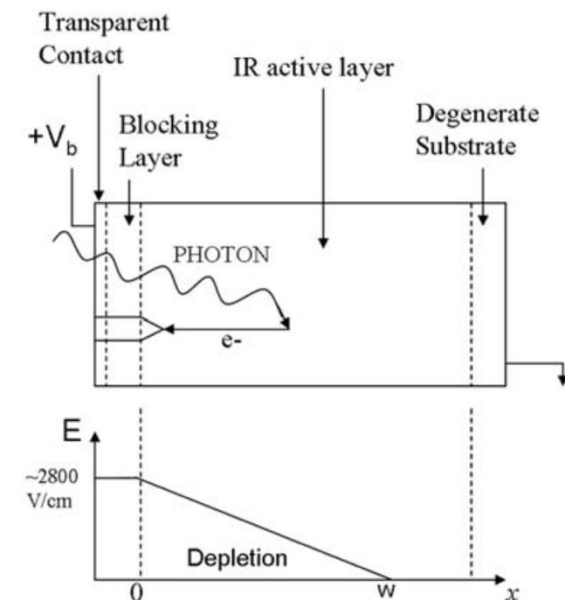


Figure 11.6. Illustration of the detection principle and operation of a typical blocked impurity band (BIB) or impurity band conduction (IBC) device.

11.3.4 Impurity band conduction devices

- Mid-IR arrays
 - 256x256, 320x240, 1024x1024 extrinsic (\leftrightarrow pure) silicon devices from Raytheon
 - 256x256, 1024 extrinsic silicon BIB detectors from DRS Technologies
 - The largest : 1K x 1K Aquarius Si:As IBC detector for 5-28 μ m
 - Pixel size : 30 μ m
 - Well : 1M or 15M electrons
 - Frame rates : 150Hz with 64 outputs
 - Pixel rates : 3MHz
 - Input-referred noise : < 1000e⁻ rms
 - QE > 40% with AR coating
 - Operated at 8-10K
 - 1K x 1K Si:As from DRS Technologies

11.3.5 Far-infrared arrays based on germanium

- The wavelength $> 40\mu\text{m}$
- There are no appropriate shallow dopants for silicon $>$ extrinsic **Ge** used
- many problems with the use of Ge
 - To control dark current, the material must be relatively lightly doped $>$ therefore absorption lengths become long (3-5mm).
 - The diffusion lengths are also large (250-300 μm)
 - $>$ pixel dimensions of 500-700 μm are required to minimize crosstalk. $>$ vulnerable to cosmic ray.
 - Because of small energy bandgaps, **these detectors must operate at liquid He temperatures well below** the silicon “freeze-out” range.
- Despite all these challenges, a 32x32-pixel Ge:Ga array was successfully developed for the 70mm band of the MIPS instrument on the Spitzer infrared space telescope.

11.3.5 Far-infrared arrays based on germanium

- Illuminating the detector pixels edge-wise
 - > satisfies the long absorption path
- The readout circuitry is stacked behind the detectors.
 - > Z-stack or Z-plane construction
- The PACS instrument on the Herschel will have a similar $70\mu\text{m}$ array like MIPS.
- AKARI satellite used a similar array stressed Ge:Ga detectors for a band at $160\mu\text{m}$.

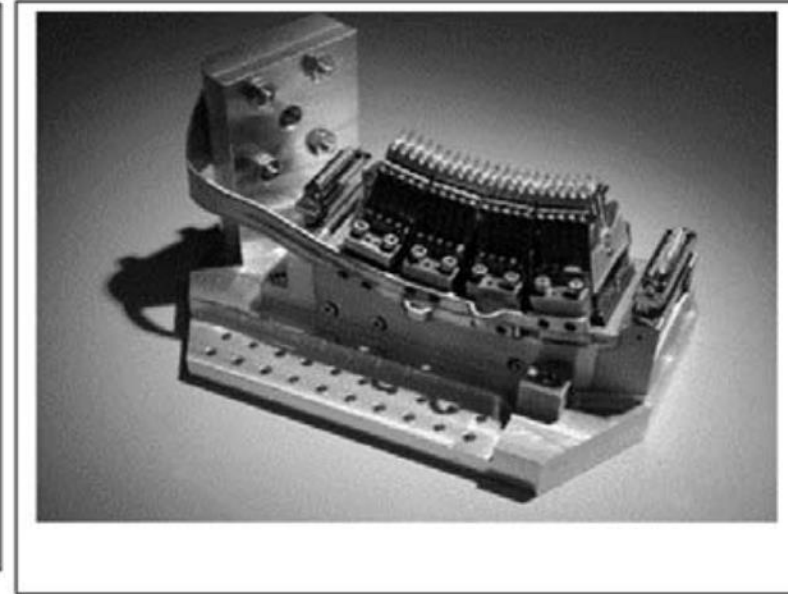
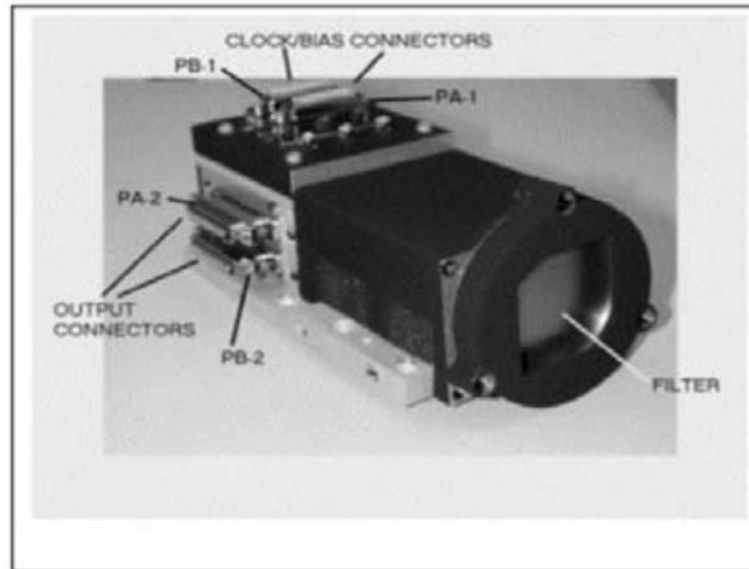


Figure 11.7. The Ge:Ga arrays used in the MIPS instrument in Spitzer. Credit: Erick Young.

11.3.6 Other forms of infrared arrays

- Platinum silicide (PtSi) array
 - PtSi is contact with p-type silicon.
 - The barrier height ψ is determined by the contact potential and can be **less than the semiconductor bandgap**.
 - PtSi, $\psi = 0.22\text{eV}$, $\lambda_c = 5.6\mu\text{m}$
 - Typical QE : less than 2-3%
 - too low compared with HgCdTe
 - These devices can be made large and uniform
 - It is all-silicon process
 - They are not as expensive as InSb or HgCdTe

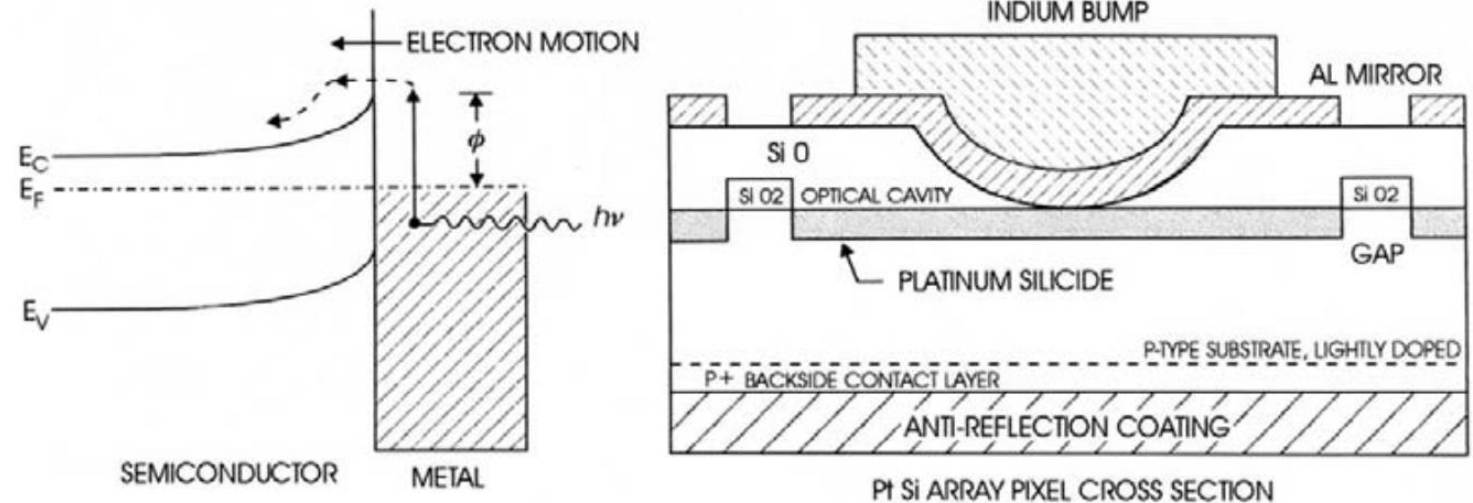


Figure 11.8. Principle of the platinum silicide (PtSi) device and the formation of a Schottky Barrier.

11.4 PRACTICAL OPERATION OF INFRARED ARRAYS

- IR arrays require a set of clock voltages to collect remove charges. and..
 - Output signals (a few $\mu\text{V}/e^-$) must be amplified
 - Digitized into data numbers
 - Pixel-to-pixel variations must be corrected
 - kTC reset noise must be eliminated.
 - Dark current must be minimized by cooling

11.3	Infrared array detectors	393
11.3.1	The infrared “array” revolution, <i>déjà vu</i>	393
11.3.2	The hybrid structure	397
11.3.3	Photovoltaic devices	400
11.3.4	Impurity band conduction devices	401
11.3.5	Far-infrared arrays based on germanium	403
11.3.6	Other forms of infrared arrays	404
11.4	Practical operation of infrared arrays	405
11.4.1	Linearity	405
11.4.2	Dark current and cooling	406
11.4.3	Noise sources	407
11.4.4	Quantum efficiency	408
11.4.5	Multiple outputs	408
11.4.6	Array controllers	408
11.5	Readout modes	410
11.5.1	Single-sampling	412
11.5.2	Correlated double-sampling (CDS)	413
11.5.3	Reset-read-read or Fowler sampling	413
11.5.4	Sampling up the ramp (UTR)	415
11.6	Infrared instruments	415
11.6.1	General issues	415
11.6.2	IR cameras	416
11.6.3	Infrared spectrometers	417
11.6.4	AO cameras and integral field spectroscopy	419
11.7	The impact of infrared arrays	420
11.7.1	Ground-based observing	420
11.7.2	The Stratospheric Observatory for Infrared Astronomy	421
11.7.3	IR astronomy in space	423

11.4.1 Linearity

- Two sources of capacitance
 - pn detector junction (C_{det})
 - The source follower FET (C_{FET})
 - (Other stray capacitances)
- Two sources of current to drive the discharge of the capacitances
 - Photoelectrons
 - Dark current electrons
- There is an obvious potential for **non-linearity between photon flux and output voltage** in the photovoltaic detectors
 - Because detector capacitances are not fixed, but depend on the width of the pn depletion region, which in turn depends on the value of the reverse bias voltage. (the effect of depletion depth for CCD is small.)
- The bias voltage changes continuously as the cell integrates.

11.4.1 Linearity

Using $Q = C(V)V$

$$dQ = \left(C + \frac{\partial C}{\partial V} V \right) dV \equiv I_{det} dt$$

- The rate of change of voltages with time (dV/dt) is **not linear** with detector current I_{det} because of the term $\frac{\partial C}{\partial V}$
- Representing all fixed capacitances as C_{fix}

$$C + \frac{\partial C}{\partial V} V = C_{fix} + C_0 \left(\left(1 - \frac{V}{V_{bi}} \right)^{-\frac{1}{2}} + \frac{1}{2} \frac{V}{V_{bi}} \left(1 - \frac{V}{V_{bi}} \right)^{-3/2} \right)$$

$$C_0 = A_{det} \left(\frac{e \epsilon_s}{2 V_{bi} \left(\frac{1}{N_A} + \frac{1}{N_D} \right)} \right)^{1/2}$$

$$V_{bi} = \frac{kT}{e} \ln \left(\frac{N_A N_D}{n_i^2} \right)$$

C_0 : junction capacitance at zero bias.
 A_{det} : is the detector area
 N_A, N_D : the acceptor and donor doping concentrations (atoms/cm²)
 ϵ_s : the permittivity of the material in the junction

11.4.1 Linearity

$$\left(\frac{dV}{dt}\right)^{-1} \propto C + \frac{\partial C}{\partial V} V = C_{fix} + C_0 \left(\left(1 - \frac{V}{V_{bi}}\right)^{-\frac{1}{2}} + \frac{1}{2} \frac{V}{V_{bi}} \left(1 - \frac{V}{V_{bi}}\right)^{-\frac{3}{2}} \right)$$

$$V \sim V_{bi}$$

$$\left(\frac{dV}{dt}\right)^{-1} \sim \infty$$

$$\frac{dV}{dt} \sim 0$$

- The line gets flat as the signal accumulates.

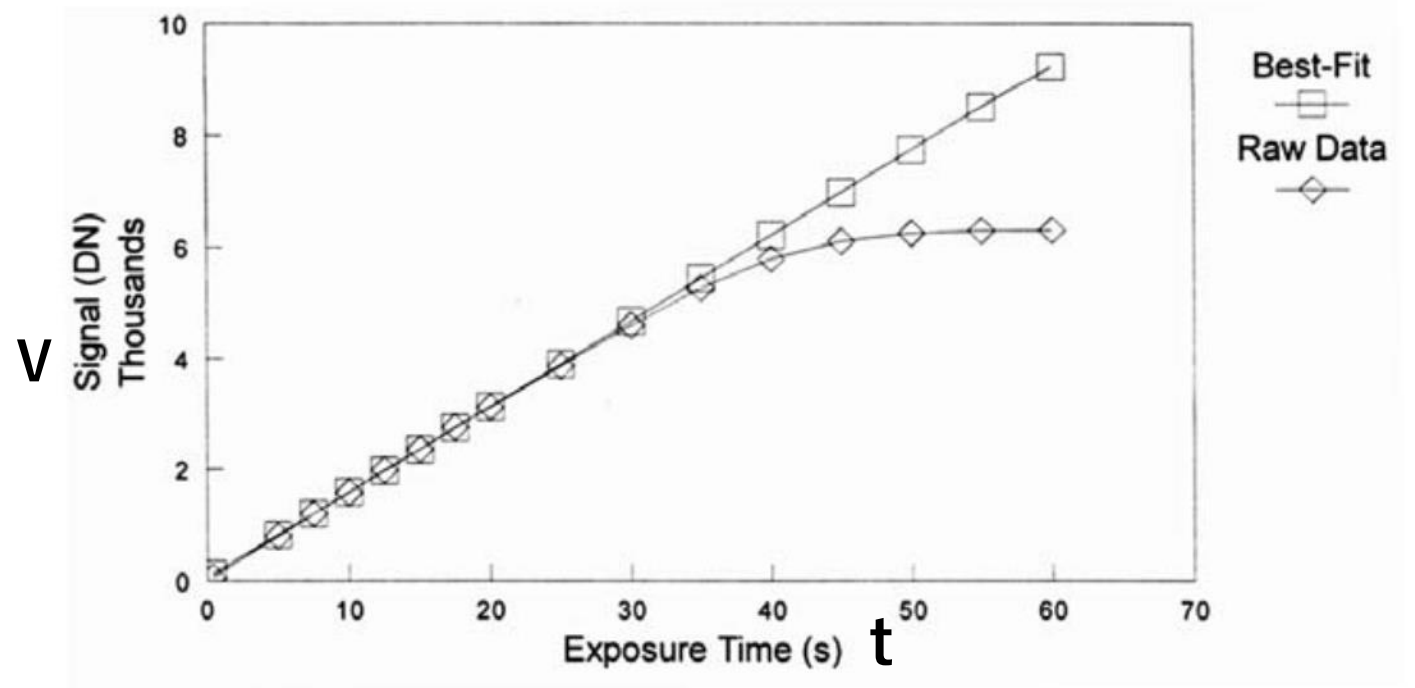


Figure 11.9. The non-linearity of an NIR array due to the voltage dependence of junction capacitance.

11.4.2 Dark current and cooling

- Three main sources of dark current
 - Diffusion
 - Thermal generation-recombination (G-R) of charges within the semiconductor
 - strong (exponential) functions of temperature
 - **Dramatically reduced by cooling**
 - Leakage currents
 - Determined by manufacturing and applied voltages

$$I_{dark} = \frac{kT}{eR_{0diff}} \left(\exp\left(\frac{eV}{kT}\right) - 1 \right) + \frac{2kT}{eR_{0GR}} \left(1 - \frac{V}{V_{bi}} \right)^{\frac{1}{2}} \left(\exp\left(\frac{eV}{2kT}\right) - 1 \right) + I_{leak}$$

V : the voltages across the detector

R_{0GR} , R_{0diff} : the detector impedances at zero bias

- $10^5 \Omega$ at 140K, $10^{10} \Omega$ at 77K for InSb detectors

Thermal voltage : $kT/e = 4.3\text{mV}$ at 50K \ll typical bias values ($V > 100\text{mV}$)

- $\exp(eV/kT) \gg 1$

11.4.2 Dark current and cooling

$$I_{dark} = \frac{kT}{eR_{0_{diff}}} \left(\exp\left(\frac{eV}{kT}\right) - 1 \right) + \frac{2kT}{eR_{0_{GR}}} \left(1 - \frac{V}{V_{bi}} \right)^{\frac{1}{2}} \left(\exp\left(\frac{eV}{2kT}\right) - 1 \right) + I_{leak}$$

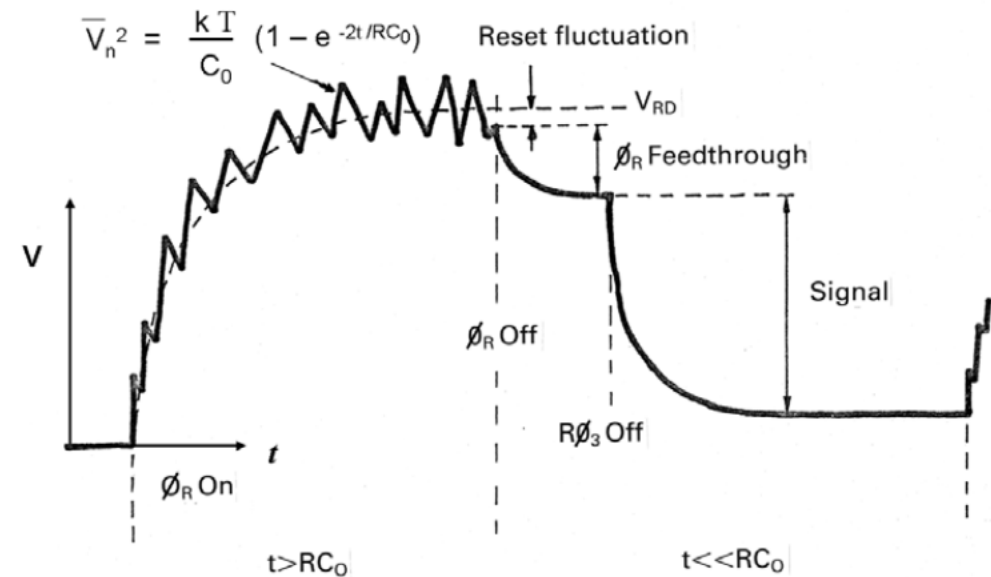
- Diffusion dominates at high temperature
- G-R contribution is dominated below 100K ($< (e^x - 1)/x$ で考えるとノイズは大きくなる気がするが、Rが温度の低下と共に大きくなるか))
- Typical dark current
 - HgCdTe at 77K : 1e/s/pix
 - InSb at the temperature below 30K and low bias : 0.1e/s/pix
- Maximum operating temperature

$$T_{max} = \frac{200K}{\lambda_c / \mu m}$$

- 2.5 μ m cutoff \rightarrow 80K
- 20 μ m cutoff \rightarrow 10K

11.4.3 Noise sources

- Readout noise (RON) describes random fluctuations in voltage
 - $R = CV_{noise}/e$ [electrons] (Section 8.6)
- kTC noise (reset noise)
 - Voltage noise of $\sqrt{kT/C}$
 - an equivalent charge noise of \sqrt{kTC}
 - ~ 54 electrons rms (77K, 0.07pF)
- kTC noise can be eliminated by taking the difference b/w the output voltages before and after reset. (CDS mode)



11.4.4 Quantum efficiency

- Near-IR arrays (HgCdTe, InSb) : QE > 80% with suitable AR coatings
- Mid-IR arrays : QE ~ 30-40% range dependent on operation
- For IR arrays the things below are all important in controlling QE
 - Non-uniformities in thinning
 - The quality of the passivation
 - Variations in doping density through a substrate or impurity centers in liquid phase epitaxy
- QE is a function of wavelength.
 - The absorption cross-section changes with wavelength.

11.4.5 Multiple outputs

- For IR observations, **background flux is huge.**
 - single exposure images are displayed with the flat-field pattern and bad pixels.
 - require to subtract the background
 - Nodding (the whole telescope moves) or chopping (the secondary mirror wobbles) methods are used for acquiring the subtraction image.
- Due to the high background, a variation of $\sim 1\%$ may swamp the targets.
 - Flat-field corrections must still be applied for photometry.
 - Allows the **shorter saturation times.**
- To deal with this condition IR arrays have multiple outputs.
 - 4,32,64...
 - Faster readout is available

11.4.6 Array controllers

- a “level shifter” circuit is required for some arrays such as HgCdTe and InSb.

- Basis features of controllers

- Fast (column) register clocks

- The fast register is clocked from column to column to enable every pixel in that row to be connected in turn to the output bus.

- Slow (row) register clocks

- Each row is addressed in sequence by pulsing the row register clocks.

- Reset clocks

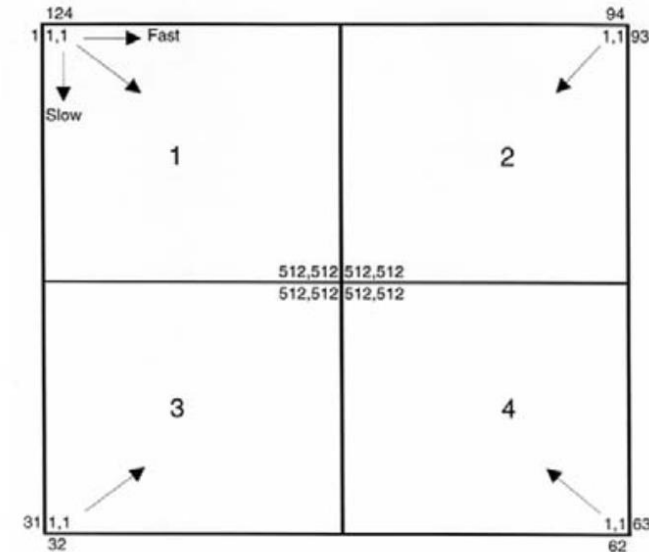
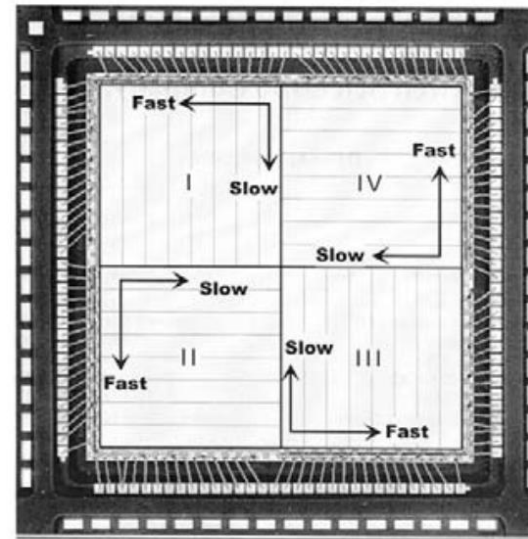
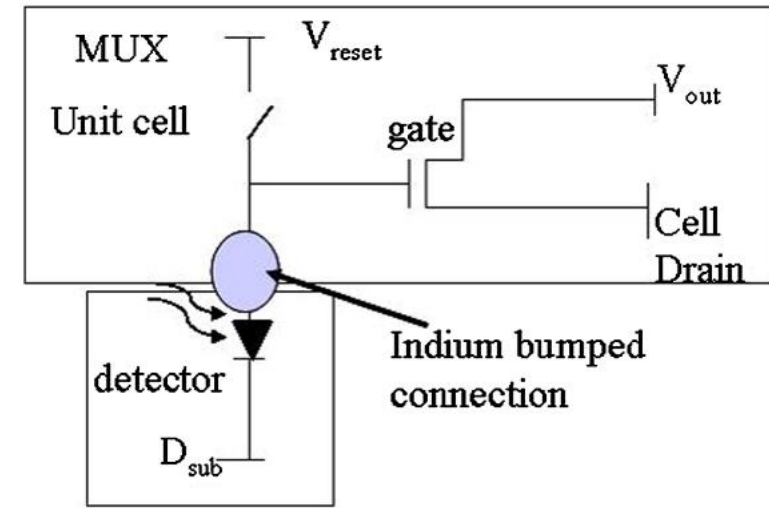


Figure 11.10. (Left) The HgCdTe 1,024 × 1,024 HAWAII array showing a readout scheme in each quadrant. (Right) The InSb 1,024 × 1,024 ALADDIN array showing the edge-to-center readout scheme.

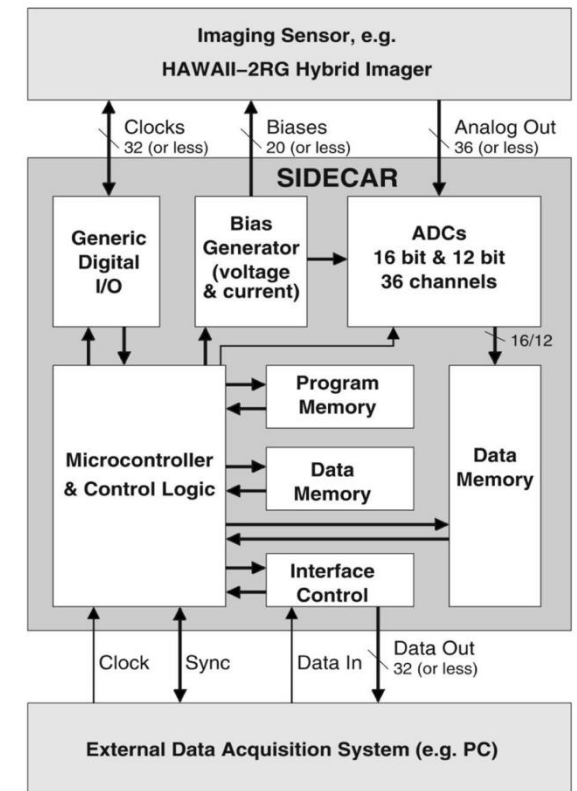
11.4.6 Array controllers

- The most important dc bias voltages
 - The substrate voltage (usually ground) and the detector substrate voltage or detector “common” supply
 - The drain voltages on the output transistor
 - The unit cell drain voltages
 - The well depth is determined by the difference between the detector substrate and the unit cell drain voltage (i.e.,
 $V_{detbias} = V_{detsub} - V_{dduc}$)
- Readout rate b/w CCDs and IR arrays
 - The pixels can fill up in a few tens of seconds for IR. -> Fast readout is needed.
 - The pre-amplifier must be decoupled to the output of the chip.
 - Higher speed electronics must be used in general. -> high system noise.



11.4.6 Array controllers

- ASICs (application-specific integrated circuits) : to achieve considerable simplification of detector electronics and reduce power consumption.
- SIDECAR
 - supplying all the clock
 - supplying bias voltages to the devices
 - digitizing the output to 16 bits before transferring the data into the host computer.



(Loose et al. 2006)

11.5 READOUT MODES

- No shutter for an IR camera to determine the exposure times.
- Instead, Most IR cameras contain a position in the filter wheel which is opaque.
- The exposure time is controlled by the sequence of reset and read pulses.
- The ability to perform a non-destructive readout for IR arrays
 - The charge in the pixel is not altered
 - Sampling the present value.

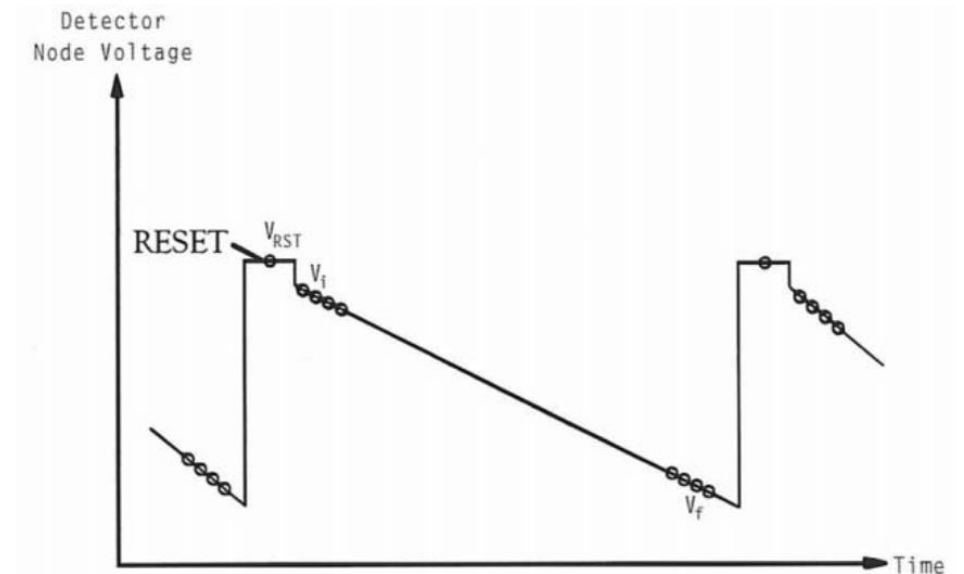
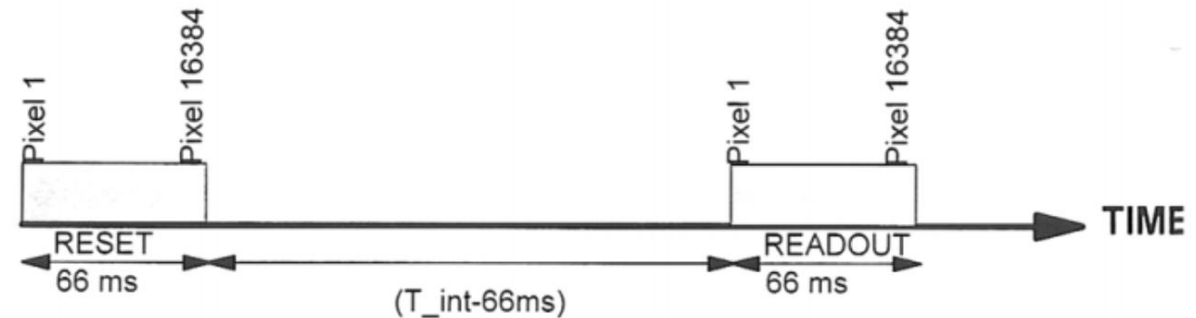


Figure 11.12. The schematic variation of the output voltage as a function of time for a typical pixel in an infrared array detector. Associated readout modes are described in the text.

11.5.1 Single-sampling

- The array must be reset.
 - to clear the detector of charge
 - to define beginning of the integration period
- Global reset / reset one row at a time
 - At the same rate as the normal readout
- Relatively timing between the "reset" wavefronts and the "readout" waveforms must be precise and stable in order.

- cons
 - Incapable of removing kTC noise and drift.
- pros
 - Directly measures the signal relative to the reset or bias level
 - Detects saturation



11.5.2 correlated double-sampling (CDS)

- Several approaches to perform CDS.
 1. To digitize the reset level in the sampling scheme already described and subtract the two results.
 2. To reset the pixel and then immediately digitize the level after the reset has been removed (the “pedestal” level) but before moving on to address the next pixel.
- Both of these approaches were common with the first IR arrays, but they turned out to be poor
 - because of strong time-dependent response to the reset action (\sim ms)
 - The act of de-addressing the current pixel adds noise.
- Better approaches are introduced in the next chapter